Original Article

The mechanism of bone metabolism in a Sprague Dawley rat model of mandibular osteoradionecrosis

Shanshan Liu[1,2#], Bin Zhang[3#], Shengnan Ma[4#], Feiguang Wu[5], Xiaona Shi[5], Jiandong Wu[6,7], Ole T. Jensen[8], Paolo Cariati[9], Jinsheng Hong[6,7], Xiaofeng Zhu[1,2]

[1]Department of Oral Maxillo-Facial Surgery, the First Affiliated Hospital, Fujian Medical University, Fuzhou, China; [2]Department of Oral Maxillo-Facial Surgery, National Regional Medical Center, Binhai Campus of the First Affiliated Hospital, Fujian Medical University, Fuzhou, China; [3]Department of Oral and Maxillo-Facial Surgery, Zhongshan Hospital Affiliated to Xiamen University, Xiamen, China; [4]Department of Oral Maxillo-Facial Surgery, People's Hospital of Tongren, Tongren, China; [5]School and Hospital of Stomatology, Fujian Medical University, Fuzhou, China; [6]Department of Radiotherapy, Cancer Center, the First Affiliated Hospital of Fujian Medical University, Fuzhou, China; [7]Key Laboratory of Radiation Biology of Fujian Higher Education Institutions, the First Affiliated Hospital, Fujian Medical University, Fuzhou, China; [8]Department of Oral Maxillofacial Surgery, University of Utah, School of Dentistry, Salt Lake City, UT, USA; [9]Department of Oral & Maxillofacial Surgery, Hospital General Universitario de Albacete, Albacete, Spain

Contributions: (I) Conception and design: X Zhu, J Hong; (II) Administrative support: S Liu, B Zhang, S Ma; (III) Provision of study materials or patients: S Liu, B Zhang, S Ma, F Wu, X Shi; (IV) Collection and assembly of data: S Liu, B Zhang, J Wu; (V) Data analysis and interpretation: S Liu, B Zhang, S Ma, X Zhu; (VI) Manuscript writing: All authors; (VII) Final approval of manuscript: All authors.

[#]These authors contributed equally to this work.

Correspondence to: Xiaofeng Zhu, PhD, MD. Department of Oral Maxillo-Facial Surgery, the First Affiliated Hospital, Fujian Medical University, No. 20 Chazhong Road, Fuzhou 350005, China; Department of Oral Maxillo-Facial Surgery, National Regional Medical Center, Binhai Campus of the First Affiliated Hospital, Fujian Medical University, Fuzhou 350210, China. Email: dentzxf@163.com.

Background: Osteoradionecrosis (ORN) is a serious complication of radiotherapy for head and neck cancer. There is currently a lack of data on the dynamic expression of genes related to bone remodeling during the development of mandibular ORN. This study aimed to establish an animal model of ORN in Sprague Dawley (SD) rats, detect the expression of genes related to bone metabolism, observe morphological changes, and clarify the mechanism of ORN.

Methods: A total of 24 male SD rats in group 1 were randomly divided into four groups (n=6/group): group a, normal control; group b, simple tooth extraction; group c, simple radiation; and group d, radiation extraction group. The right mandible of rats in groups c and d was irradiated with a single dose of 35 Gy. The right mandibles were taken from each group for morphological observation 90 days after irradiation. SD rats in group 2 (n=144) were randomly divided into four groups (in similar fashion to group 1 but with groups a', b', c', and d'). Samples were collected at six time points after irradiation. Histopathological changes were observed, and Western blotting (WB) was used to analyze protein expression.

Results: The formation of dead bone and pathological fracture was visible under micro-computed tomography (micro-CT), and tissue biopsy showed late fibrosis repair. In group d', osteogenesis and osteoclasis coexisted in the early irradiation stage. Vascular endothelial growth factor (VEGF) receptor expression was lower in groups c' and d' than in group a'. On day 45, runt-related transcription factor 2 (RUNX2) expression in group d' was lower than that in the other groups. The ratio of receptor activator of nuclear factor-κβ ligand to osteoprotegerin (RANKL:OPG) differed significantly among groups b', c', and d' on the 45th day (d' > c' > b').

Conclusions: Radiation and vascular function damage resulted in the lower expression of VEGF. The first 15 days after radiation was mainly characterized by new bone formation. After 15 days, bone resorption increased. Tooth extraction trauma can aggravate the bone metabolism imbalance and promote ORN

© Quantitative Imaging in Medicine and Surgery. All rights reserved.

occurrence. These findings shed light on the mechanism of ORN.

Keywords: Mandibular osteoradionecrosis (mandibular ORN); bone metabolism; radiotherapy

Submitted Jan 09, 2024. Accepted for publication May 06, 2024. Published online May 17, 2024.
doi: 10.21037/qims-24-47
View this article at: https://dx.doi.org/10.21037/qims-24-47

Introduction

Osteoradionecrosis (ORN) is a serious complication of radiotherapy for malignant tumors of the head and neck (1). ORN often leads to local tissue ulceration, deformity, and organ defects in the oral and maxillofacial region. In recent years, with the rapid advancement in radiotherapy equipment and technology, along with the popularization of three-dimensional conformal radiotherapy (3DCRT) in clinical practice, the incidence of ORN has decreased but is nonetheless frequent, with an incidence of 2–22% (2). The incidence of ORN in the mandible is significantly higher than that in other craniofacial bones (3), but there is no consensus regarding the etiology or pathology of mandibular ORN. However, after the 1980s, microsurgical reconstruction techniques became viable options for reconstructing the jaw defects caused by ORN. Despite this, clinical treatment is still quite problematic, and there is no effective preventive method at present; therefore, the pathogenesis of ORN remains a critical area of medical investigation (4).

Due to the extensive research on mandibular ORN regarding histopathology, cell biology, molecular biology, and genomics, novel theories such as radiation atrophy fiber chemistry and bone cell injury have received increased attention. These provide new ideas for the clinical treatment of ORN and have achieved a degree of success (5-7). Chinese scholars Wang and Zheng found that during the occurrence and development of ORN, vascular damage and abnormal bone metabolism occur (8). Past research on the pathological mechanism of mandibular ORN has mainly focused on histopathological examination and on the formation of mandibular ORN. However, there is a lack of data on the dynamic expression of bone remodeling–related genes during the occurrence and development of mandibular ORN.

In this study, an animal model of ORN in the mandible of Sprague Dawley (SD) rats was established, from which samples were taken at six time points: the 4th, 9th, 15th, 30th, 45th, and 90th day after radiation. Samples were systematically observed for histomorphological changes, and molecular methods were used to detect the dynamic expression of genes related to bone metabolism. The aim of these procedures was to clarify the possible mechanism of mandibular ORN pathogenesis and to identify target genes for the tissue engineering repair of ORN. We present this article in accordance with the ARRIVE reporting checklist (available at https://qims.amegroups.com/article/view/10.21037/qims-24-47/rc).

Methods

Experimental material

Experimental animals and grouping

A nonregistered protocol was prepared before the study. This study was reviewed and approved by the Animal Care and Use Committee of Fujian Medical University, and all experiments complied with the relevant regulations of the Experimental Animal Center of Fujian Medical University for the care and use of animals. Healthy SD male rats (specific-pathogen-free grade, 10 weeks old, body weight 400±15 g) were provided by Shanghai Slack Laboratory Animal Co., Ltd. (Shanghai, China). They were raised in the Experimental Animal Center of Fujian Medical University in a barrier system, with standard rat feed and unlimited drinking water; three rats were housed per cage for 1 week. The experiment was carried out after no abnormalities were found in rats' activity or stool. The feed, the drinking, and the bedding were each changed twice a week. A total of 24 SD rats in group 1 were randomly subdivided into the following four groups via a random number table method (n=6/group): a, normal control; b, simple tooth extraction; c, simple radiation; and d, radiation extraction. Group a was used as a control group without any intervention; rats in group b had all the molars on the right mandible extracted after 15 days; rats in group c were irradiated on the right mandible on the first day; and rats in group d were irradiated on the right mandible on the first day, 15 days after which the right mandibular molars were extracted. SD

© Quantitative Imaging in Medicine and Surgery. All rights reserved.

rats in group 2 (n=144) were randomly subdivided into four groups via random number table method (n=36/group); the grouping strategy was the same as that in group 1 but with the groups designated as a', b', c', and d'. Rats that died during the experiment were supplemented according to the original experimental conditions. After irradiation or tooth extraction, if there was occlusal disorder or infection, soft food was provided. During the experiment, animal care staff and those administering treatments remained unaware of the group allocations to ensure that all animals in the experiment were handled, monitored, and treated in the same manner.

Drugs and reagents

The following items were obtained for the study: a Masson Trichrome Staining Kit (Beijing Zhongshan Jinqiao Company, Beijing, China), hematoxylin (Xiamen Lulong Biotechnology Development Co., Ltd., Xiamen, China), eosin (Sinopharm Pharmaceutical Co., Ltd., Beijing, China); anti-receptor activator of nuclear factor-κβ (RANK) ligand (RANKL) antibody (ab45039; Abcam, Cambridge, UK), anti-osteoprotegerin (OPG) antibody (ab9986; Abcam); anti-runt-related transcription factor 2 (RUNX2) antibody (ab23981; Abcam), anti-vascular endothelial growth factor (VEGF) antibody (ab32152; Abcam), anti-glyceraldehyde-3-phosphate dehydrogenase (GAPDH) antibody (AF0006; Beyotime, Haimen, China), goat anti-rabbit horseradish peroxidase (HRP) secondary antibody (Ab6721; Abcam), and goat anti-small mouse (HRP) secondary antibody (A0216; Beyotime).

Instruments and equipment

A linear accelerator (Clinac600C/D; Varian Medical Systems Medical Corporation, Palo Alto, CA, USA), radiation therapy planning system (Pinnacle9.2; Philips, Amsterdam, the Netherlands), simulated positioner (LX-40A; Toshiba Co., Ltd., Tokyo, Japan), and micro-computed tomography (micro-CT; Skyscan 1176, Kontich, Belgium) were used in the study.

Experimental methods

Irradiation source and method

A linear accelerator was used to irradiate the right mandible of SD rats with an average energy of 6 MV-X-rays at a dose rate of 300 cGy/min. For the irradiation field, the upper boundary was the upper edge of the mandible, the lower boundary was the lower edge of the mandible, the anterior boundary was the anterior edge of the right mandibular first molar, and the posterior boundary was the posterior edge of the ascending ramus of the mandible. The linear accelerator was used for a one-time irradiation at a dose of 35 Gy. Single irradiation was performed on the right mandible in groups c, c', d, and d'. If the rats woke up from anesthesia or moved their bodies during irradiation in a manner that might have affected the irradiation effect, the rats were excluded from the experimental group.

Tooth extraction

At 15 days after irradiation, all the molars of the right mandible in groups b, b', d, and d' were extracted. Anesthesia was administered via intraperitoneal injection of 10% chloral hydrate at a dose of 0.33 mL/100 g. All extractions were performed by the same surgeon. Penicillin was routinely administered for 3 days after tooth extraction, and 20,000 units per day were injected into the muscle to prevent wound infection. From the 3rd day to the 14th day after irradiation, 3 mL of milk and feed nutrient solution was continuously injected into the stomach.

Experimental materials

After 90 days of irradiation, SD rats in group 1 were killed by cervical dislocation. Bones of the right mandibular molar area were removed and placed into the specimen box and then subjected to routine fixation, dehydration, and embedding. These specimens were used for hematoxylin and eosin (HE) and Masson examinations. SD rats (n=6/group/time point) in groups a', b', c', and d' were killed at six time points on the 4th, 9th, 15th, 30th, 45th, and 90th day after irradiation. Tissues used for quantitative Western blotting (WB) were directly labeled and stored in liquid nitrogen.

Observation indicators

Micro-CT inspection analysis

Micro-CT was performed regularly to observe the bone density and bone destruction of the right mandible of SD rats before and after irradiation. SD rats were placed in a supine and fixed on a wooden board. After 90 days of irradiation, SD rats in group 1 were killed, and the right mandible was removed, fixed with 4% paraformaldehyde for 3 days, and scanned by micro-CT.

HE staining

The fixed bone specimens were reduced to 3- to 5-mm bone blocks and placed in 10% ethylenediaminetetraacetic acid

© Quantitative Imaging in Medicine and Surgery. All rights reserved.

(EDTA) for decalcification. The solution was decalcified until the specimens could be gently penetrated with a pin. The tissues were then paraffin-embedded, and paraffin blocks were cut into serial sections with a thickness of 4 μm using a microtome and subjected to conventional HE staining.

Masson trichrome staining

Paraffin sections were deparaffinized and rehydrated, stained with Weigert's iron hematoxylin solution for 8 minutes, rinsed with Masson Ponceau acid solution for 8 minutes, stained with Aniline blue for 5 minutes, dehydrated, and then sealed with neutral glue.

Evaluation of pathological tissues

Photos were taken under an optical microscope. The specific targets of VEGF, RUNX2, OPG, and RANKL in SD rat samples were effectively screened by WB, and their expression levels were detected.

The extracted tissues were cut into fragments on ice, and radioimmunoprecipitation assay (RIPA; lysate) and phenylmethylsulfonyl fluoride (PMSF; protease inhibitor) were added. The supernatant was transferred to a new centrifuge tube to obtain the total tissue proteins. According to the concentration of each protein sample, 80 μg of the same quality sample was obtained, and the electrophoresis was stopped when the loading buffer reached the bottom edge of the gel. Proteins were then transferred to polyvinylidene fluoride (PVDF) membranes and stained via immunohistochemical reaction.

Statistical analysis

SPSS 20.0 (IBM Corp., Armonk, NY, USA) was used for statistical analysis. When the data conformed to a normal distribution, the comparison between the means of multiple groups was performed using a single-factor analysis of variance. The results are expressed as the mean ± standard deviation. If the data did not conform to normal distribution, the Wilcoxon rank-sum test was applied. $P<0.05$ was considered statistically significant.

Results

Ninety-day micro-CT imaging findings in group 1

In group a, the bone density of the right mandible was normal, and there was no bone defect or pathological fracture (*Figure 1A*). In group b, the bone restoration of the mandibular extraction wound in the right molar area was normal (*Figure 1B*). In group c, the bone density in the right mandibular molar area was normal, but there were evident imaging changes (*Figure 1C*). In group d, bone defects and low density appeared in the molar area of the right mandible, which were accompanied by pathological fractures (*Figure 1D*).

HE staining results in group 1 samples

In group a, the cortical bone cells were arranged neatly, the lamellar structure was clear, and there were few blank bone lacunae (*Figure 2A*). In group b, the bone marrow cavity and bone cortex of the molar area of the right mandible had no significant differences compared with group a (*Figure 2B*). In group c, there was bone marrow cavitation of the irradiated molars, mild inflammatory cell infiltration, disorder of the cortical bone cells, and mild fibrosis of the intercellular substance (*Figure 2C*). In group d, the degree of cortical necrosis was further aggravated, sequestered bone was present, a large amount of fibrous tissue was seen in the bone defect area, and a large number of blank bone lacunae were visible in the cortical bone (*Figure 2D*).

Analysis of Masson results in group 1 samples

In group a, there was no fibrous tissue hyperplasia in the bone marrow cavity (*Figure 2E*). In group b, there was no significant difference from the blank control group and no fibrous tissue hyperplasia in the bone marrow cavity (*Figure 2F*). In group c, a small amount of fibrous tissue was observed in the bone marrow cavity 90 days after radiation, and the integrity of the bone marrow cavity was clear (*Figure 2G*). In group d, a large amount of fibrous tissue was found in the bone marrow cavity 90 days after irradiation, and a complete anatomic shape of the bone marrow cavity was absent (*Figure 2H*).

HE staining results in group 2 samples

In the normal mandible, bone cells were arranged neatly, and the lamellar structure was clear (*Figure 3A*); 4 days after irradiation, inflammatory cells and multinucleated osteoclasts could be observed in the Haversian canals (*Figure 3B*). At 9 days, osteoclast bone lacunae were apparent in the Haversian canal, the cavity of the Haversian canal became enlarged, and a pink amorphous necrotic

© Quantitative Imaging in Medicine and Surgery. All rights reserved.

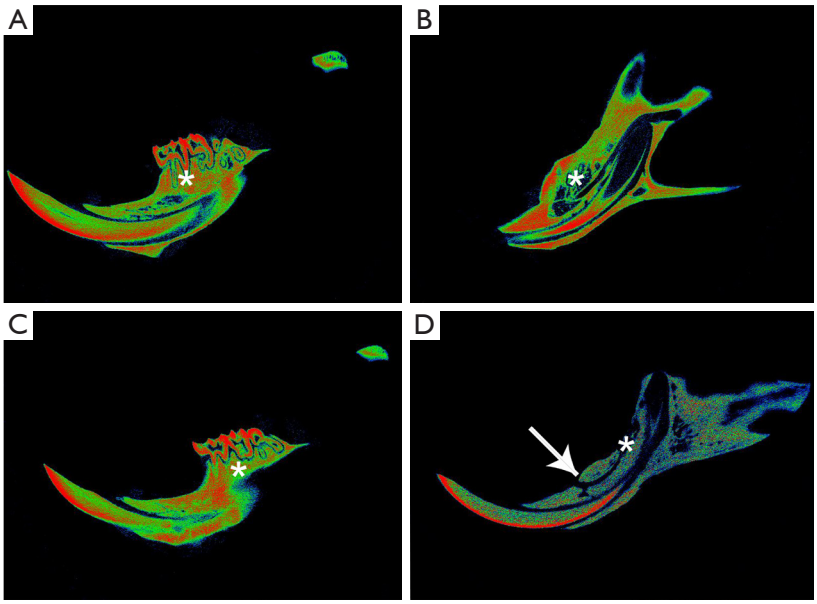

Figure 1 Micro-CT imaging at 90 days (the higher the density, the closer to red; the lower the density, the closer to black). Bone density in the molar area of the right mandible in groups (A) a, (B) b, and (C) c appeared normal (*). (D) Bone defect (*) appeared in the right mandibular molar area in group d, the density was significantly reduced, and pathological fractures (arrow) were apparent. Micro-CT, micro-computed tomography.

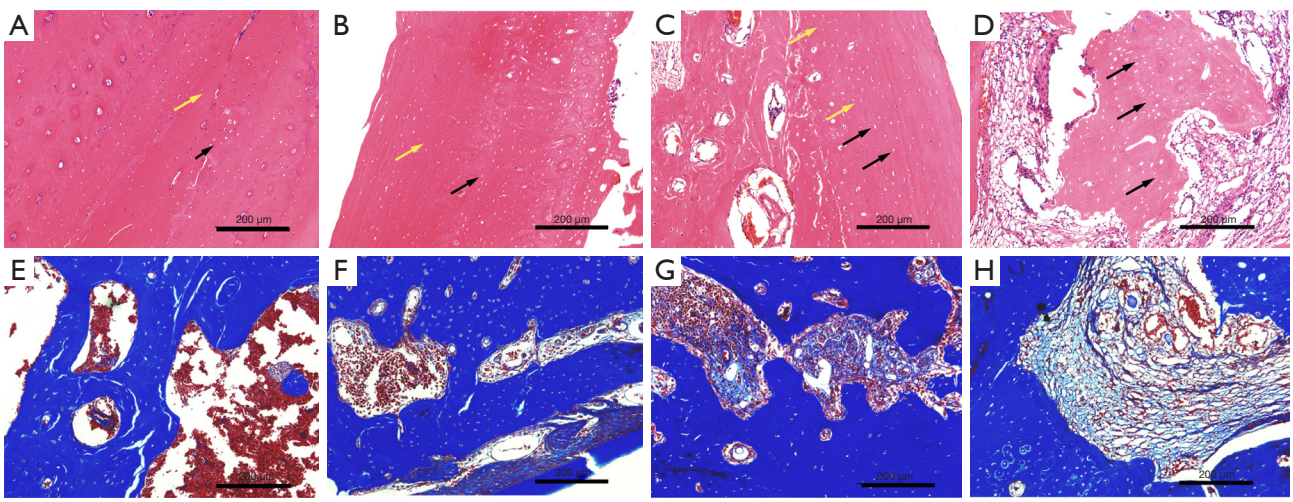

Figure 2 Histopathological changes in the mandible of SD rats in the different groups. (A-D) Histopathological changes in HE staining of the right mandible at 90 days. (E-H) Histopathological changes according to Masson staining in the bone marrow cavity of the right mandible at 90 days. (A) Bone cortex of group a, including blank bone lacunae (black arrow) and bone lacuna bone cells (yellow arrow). (B) Group b (simple extraction group): bone cortex, including blank bone lacunae (black arrow) and bone lacuna bone cells (yellow arrow); there was no significant difference compared with the normal control group. (C) In the bone cortex of group c, the number of blank bone lacunae (black arrows) and bone lacuna bone cells (yellow arrows) increased significantly. (D) Bone cortex, blank bone lacunae (black arrows), freeing of dead bone, and a large amount of surrounding fibrous tissue filling the bone defect area in group d. (E) The bone marrow cavity in group a, with no fibrous tissue hyperplasia. (F) No fibrous tissue proliferation apparent in group b. (G) A small amount of fibrous tissue in the marrow cavity in group c, with the integrity of the marrow cavity being maintained. (H) No integrity of the marrow cavity in group d, with a large amount of fibrous tissue. SD, Sprague Dawley; HE, hematoxylin and eosin.

© Quantitative Imaging in Medicine and Surgery. All rights reserved.

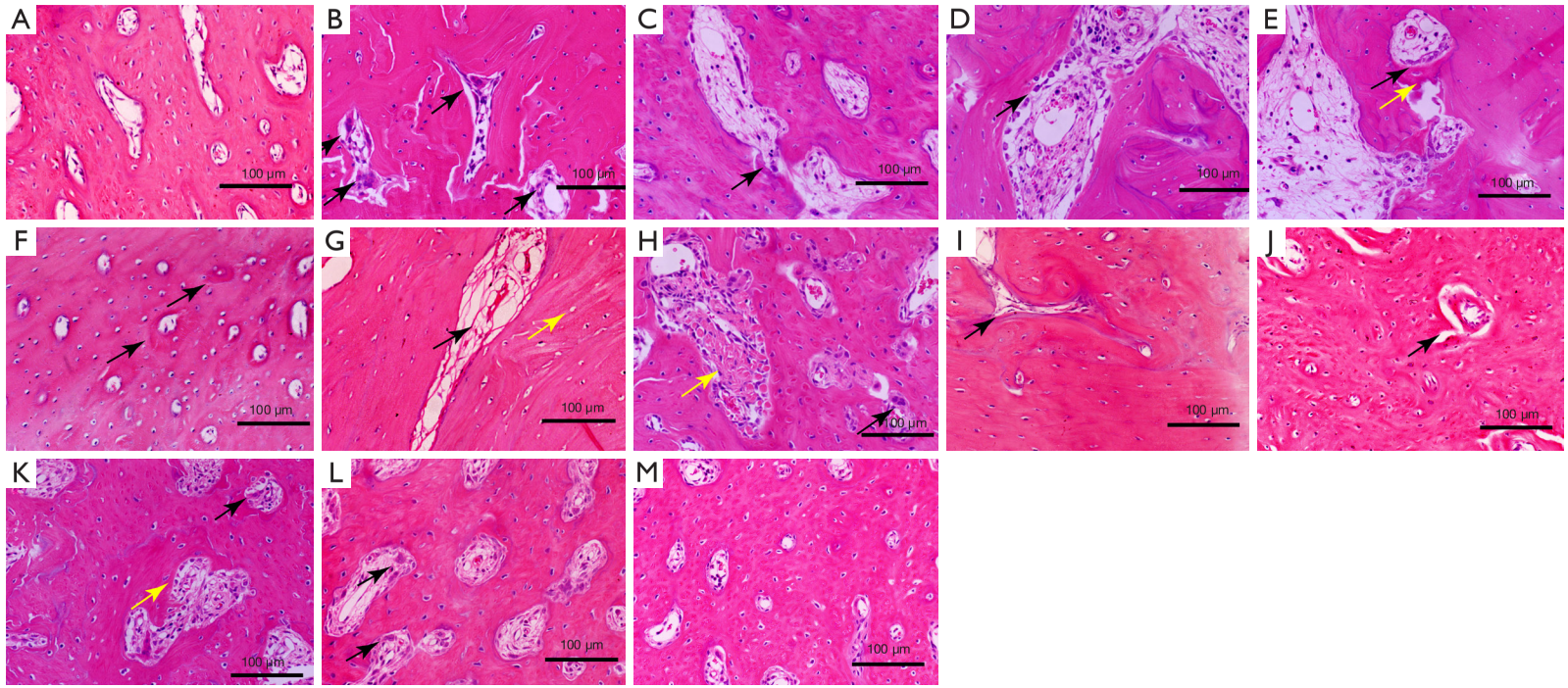

Figure 3 The histopathological changes on HE staining of normal control group a', simple tooth extraction group b', simple radiation group c', and radiation extraction group d'. (A) Normal lamellar bone. (B) At 4 days in the radiation extraction group, inflammatory cells and multinucleated osteoclasts appeared in Haversian canal (black arrows). (C) At 9 days in radiation extraction group, Haversian canal osteoclast lacunae (black arrow), enlargement of the Haversian canal, and pink amorphous necrotic material appeared. (D) At 15 days in the radiation extraction group, osteoclast bone resorption disappeared, osteoblasts appeared to adhere to the bone surface (black arrow), and smaller amount of bone deposition in the matrix were observed. (E) At 30 days in the radiation extraction group, bone surface osteoblast adhesion decreased (yellow arrow) and a greater amount of bone deposition was apparent in the Haversian canal (black arrow). (F) At 45 days in the radiation extraction group, the number of osteoblasts decreased, and small changes in Haversian canal were apparent, with a greater amount of peritubular indeterminate necrotic material (black arrows). (G) At 90 days in the radiation extraction group, the number of osteoblasts was significantly reduced, Haversian canal was enlarged, fibrous tissue was packed (black arrow), and the number of bone lacunae were significantly increased (yellow arrow). (H) At 30 days in the simple radiation group, the number of osteoblasts increased, osteoclasts were visible, cell adhesion on the bone surface, and erythrocytes (black arrow) and osteoclasts (yellow arrow) overflowing the blood vessels could be observed locally. (I) At 45 days in the radiation only group, the number of osteoblasts decreased, bone-crushing phenomenon remained visible, a small number of cells appeared to be attached to the Haversian canal (black arrow), and the lumen was enlarged. (J) At 90 days in the radiation-only group, the number of bone lacunae was reduced, no osteogenesis or osteoclasts was apparent, and the area of the Haversian canal was heterogenous, with indeterminate necrotic material (black arrow) and a small degree of cell infiltration in the lumen. (K) At 30 days in the simple extraction group, the lumen of the Haversian canal appeared slightly enlarged, with osteoblasts (black arrow) and osteoclasts (yellow arrow) adherent to the bone surface. (L) At 45 days in the simple extraction group, the lumen of the Haversian canal was enlarged, and a large amount of bone formation (black arrows) and osteoclast infiltration was visible in the lumen. (M) The simple tooth extraction group at 90 days. HE, hematoxylin and eosin.

© Quantitative Imaging in Medicine and Surgery. All rights reserved.

material appeared (*Figure 3C*). At 15 days, osteoclast bone resorption ceases, and bone formation appeared on the bone surface. Cell adhesion showed that a small portion of bone was deposited in the matrix (*Figure 3D*). At 30 days, osteoblast adhesion on the bone surface was reduced in group d', and more bone deposits appeared in the Haversian canal (*Figure 3E*). At 45 days, the tissue imaging of group d' showed that the lumen in the Haversian canal was smaller and that the amount of surrounding necrotic material had increased (*Figure 3F*). At 90 days, the histology of group d' showed that the lumen in the Haversian canal was packed with fibrous tissue. The cavity was enlarged, and the number of bone lacunae was considerably increased (*Figure 3G*). At 30 days, bone surface cell adhesion was observed in group c' (without tooth extraction), and erythrocytes and osteoclasts overflowing blood vessels were visible locally (*Figure 3H*). At 45 days after irradiation, a small number of cells in the Haversian canal of group c' appeared to be attached and the lumen enlarged (*Figure 3I*). At 90 days, amorphous necrotic material appeared in different degrees around Haversian canals, and a small amount of cell infiltration was visible in the lumen (*Figure 3J*). In group b', at 30 days (i.e., 15 days after tooth extraction), mild expansion of the lumen of the Haversian canal and adhesion of osteoblasts and osteoclasts could be seen on the bone surface (*Figure 3K*). Additionally, 30 days after tooth extraction, the lumen of the vessels in Haversian canals was enlarged, and a large amount of osteoblast and osteoclast infiltration was visible in the lumen (*Figure 3L*). In tissues at 90 days (75 days after tooth extraction), there was no evident change as compared to the normal mandible (*Figure 3M*).

Detection of VEGF, RUNX2, OPG, and RANKL expression levels in group 2

VEGF, RUNX2, OPG, RANKL, and RANKL:OPG expression in the simple tooth extraction group (group b')

There was no significant difference in VEGF expression at 30, 45, and 90 days in group b' compared with that in the control group. RUNX2 expression in group b' did not significantly differ from that in the control group at 30 and 90 days, and it was considerably higher than that in the control group at 45 days ($P<0.01$). OPG expression in group b' was lower than that in the control group at 30 days and was considerably higher than that in the control group at 45 and 90 days. Protein factor RANKL expression was higher in group b' than in the control group at 45 days, but at 30 and 90 days, there was no significant difference compared with the normal control group. The RANKL:OPG ratio in group b' was considerably higher than that in the control group at 30 days but was lower than that in the control group at 45 and 90 days. There was no significant difference in RANKL:OPG ratio between 45 and 90 days (*Figure 4*).

VEGF, RUNX2, OPG, RANKL, and RANKL:OPG expression in the simple radiation group (group c')

VEGF expression in group c' was lower than that in the control group, and there was no statistical difference between the groups. RUNX2 expression on the 4th, 9th, and 30th day after radiation was considerably higher than that in the control group, and there was no significant difference between the three time points ($P<0.001$). Although the expression levels at 15, 45, and 90 days in group c' were not significantly different from those in the control group, OPG and RANKL expression in group c' first increased and then gradually returned to normal. Furthermore, the RANKL:OPG ratio in group c' was higher than that in the control group at 45 days, and there was no significant difference compared with the control group at 15 and 30 days. The RANKL:OPG ratio in group c' was lower than that in the control group at 4 and 9 days (*Figure 5*).

VEGF, RUNX2, OPG, RANKL, and RANKL:OPG expression in group d'

VEGF expression was lower in group c' than in group a', and there was no significant difference in the expression between each time point. RUNX2 expression in group d was considerably different around 15 days after radiation and gradually increased at 4 days ($P<0.001$). It reached a peak at 9 days, which was significantly higher than that in the control group, and then rapidly dropped to a normal level until 90 days. OPG expression at 4, 9, 15, and 90 days was higher than that in group a' at 30 and 45 days. RANKL expression in group d' was considerably lower than that in the control group; RANKL expression at 4, 9, and 90 days was not significantly different from that in the control group but was considerably elevated compared with that in the control group at 15 and 30 days. RANKL:OPG ratio showed a gradual increase and then decreased, peaking at 45 days. The ratio on 30 and 45 days was considerably higher than that in the control group, and the ratios at the other 4 time points were considerably lower than those in the control group (*Figure 6*).

© Quantitative Imaging in Medicine and Surgery. All rights reserved.

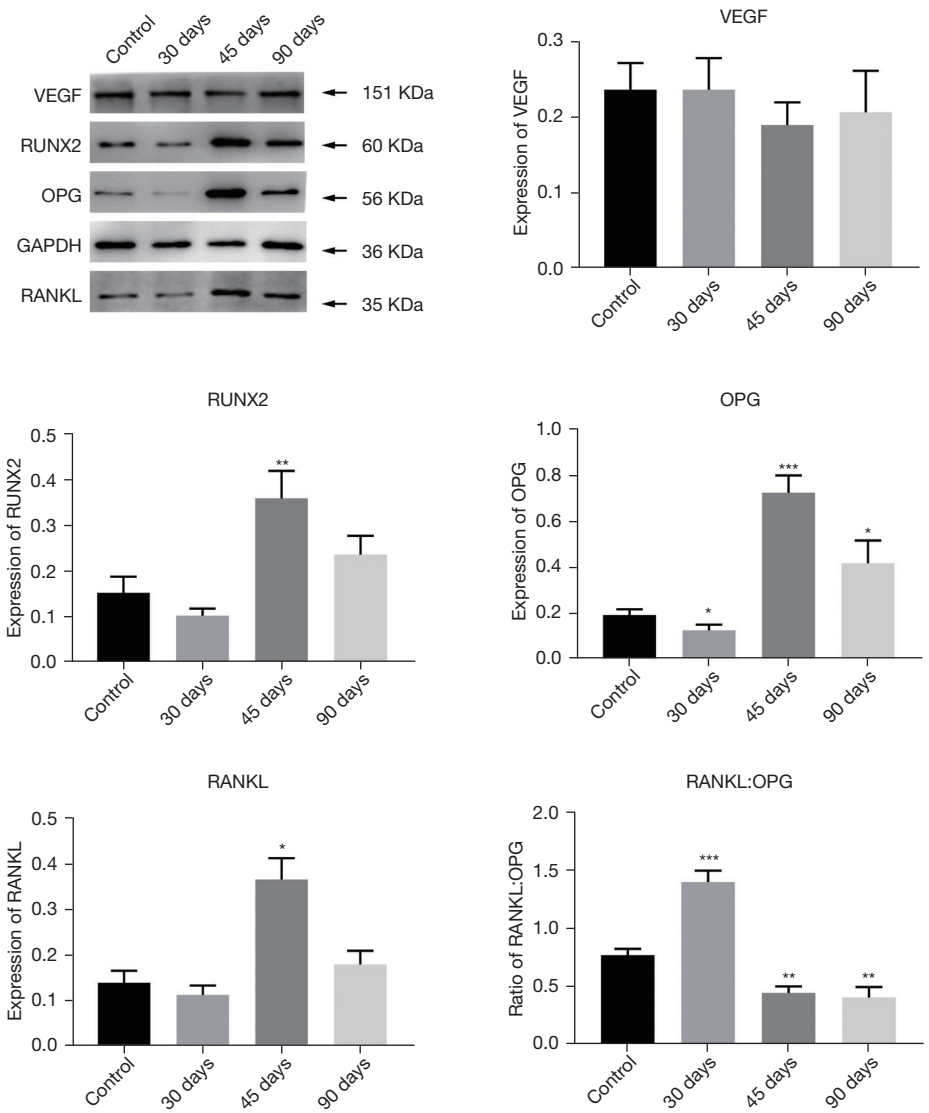

Figure 4 WB detection of VEGF, RUNX2, OPG, and RANKL expression and the RANKL:OPG ratio at different time points in group b'. *, P<0.05; **, P<0.01; ***, P<0.001. VEGF, vascular endothelial growth factor; RUNX2, runt-related transcription factor 2; OPG, osteoprotegerin; GAPDH, glyceraldehyde-3-phosphate dehydrogenase; RANKL, receptor activator of nuclear factor-κβ ligand; WB, Western blotting.

Discussion

Reliability of the SD rat ORN animal model

The formation of not only dead bone and pathological fractures was observed by micro-CT. Histopathological staining showed that the lamellar bone was broken, the bone cells had disappeared, and the fibrosis was later repaired. This study provides evidence of the occurrence of mandibular ORN from various angles and demonstrates the reliability of the modeling method used (9).

Changes in VEGF expression in ORN of the mandible

A variety of cells in bone tissue can express VEGF, especially bone marrow mesenchymal stem cells (BMSCs) and osteoblasts (10). VEGF is a key paracrine factor for angiogenesis and a factor for vascular renewal and metabolism, playing a key role in the balance of bone metabolism (11). VEGF can adjust the balance of osteoblast and adipocyte differentiation of BMSCs by regulating the level of RUNX2, a specific transcription factor of

© Quantitative Imaging in Medicine and Surgery. All rights reserved.

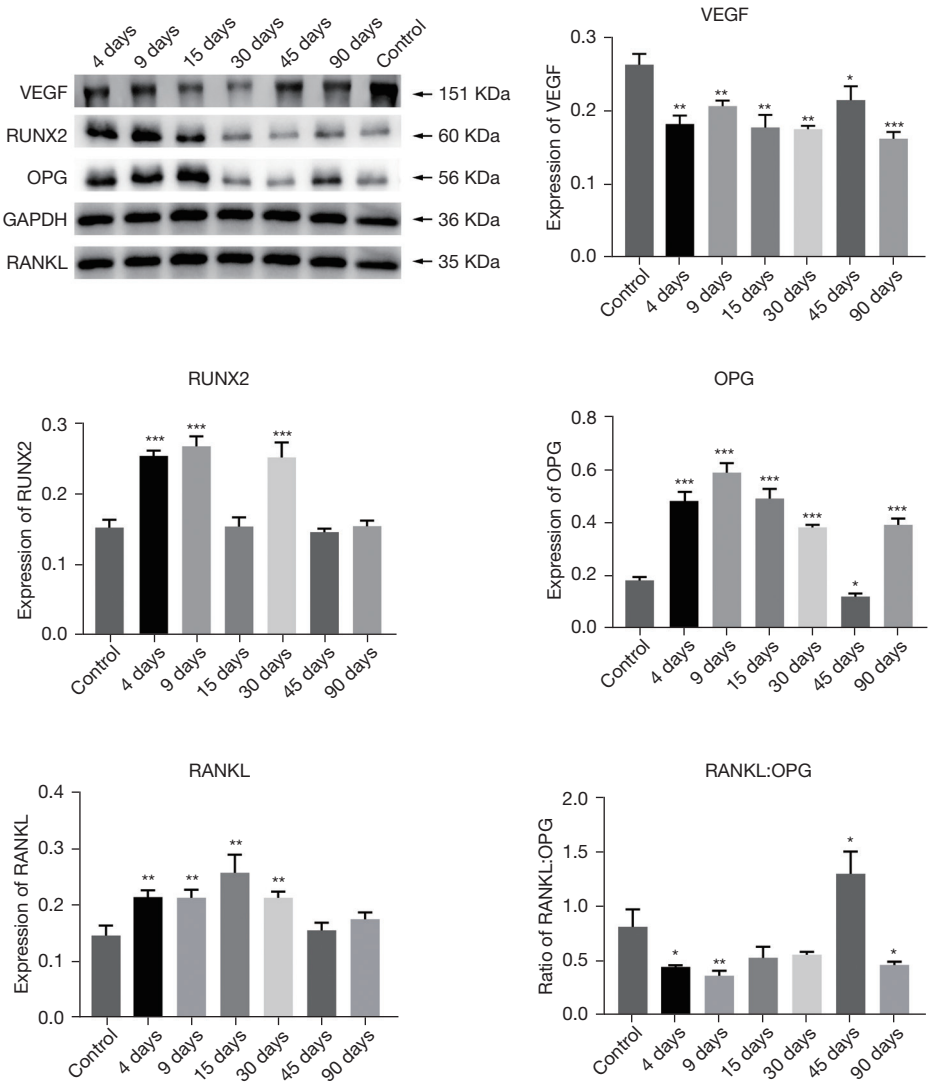

Figure 5 WB detection of VEGF, RUNX2, OPG, and RANKL expression and the RANKL:OPG ratio at different time points in group c'. *, P<0.05; **, P<0.01; ***, P<0.001. VEGF, vascular endothelial growth factor; RUNX2, runt-related transcription factor 2; OPG, osteoprotegerin; GAPDH, glyceraldehyde-3-phosphate dehydrogenase; RANKL, receptor activator of nuclear factor-κβ ligand; WB, Western blotting.

osteoblasts, to control the increase or decrease in bone mass and regulate the balance of bone metabolism (10). Studies have shown that changes in bone vascular metabolism following radiation are mainly reflected in the blockage of local vascular renewal, metabolic stagnation, and impaired function, yet the number and density of blood vessels do not decrease, and even in the early stage of radiation, the blood flow of the jaw increases rather than decreasing (8,12,13).

In our study, VEGF expression decreased in groups c' and d' at each time point and was lower than that of groups a' and b', in which irradiation was not performed. The obvious local vascular disintegration observed via HE staining in groups c' and d' further demonstrated that the bone blood flow in the radiation area was not affected, but the local vascular function was degraded. After irradiation, VEGF expression in groups c' and d' were lower than that in the control group. At 4, 9, and 15 days, RUNX2 expression, which is closely related to osteoblasts, was significantly higher in groups c' and d' than in the nonirradiated groups a' and b'. It is speculated that the dysfunction of BMSCs

© Quantitative Imaging in Medicine and Surgery. All rights reserved.

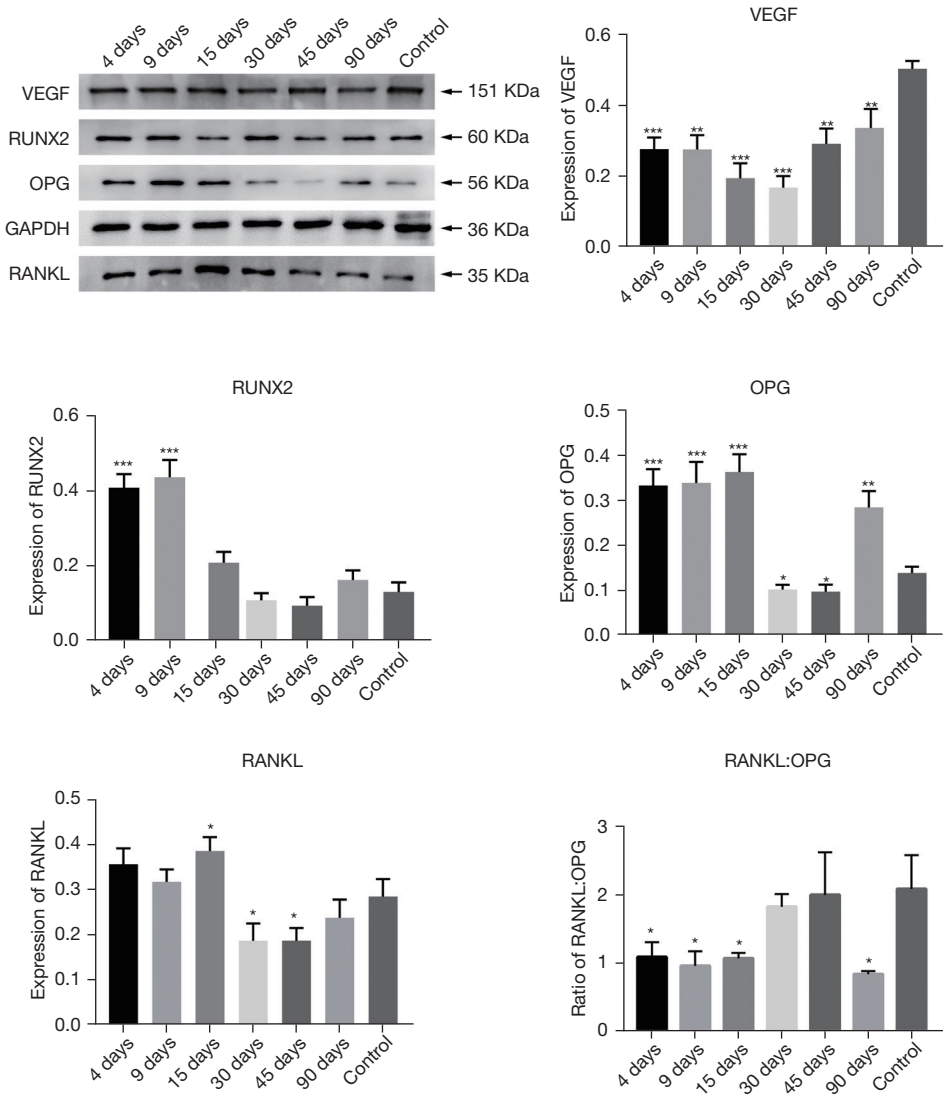

Figure 6 WB detection of VEGF, RUNX2, OPG, and RANKL expression and the RANKL:OPG ratio at different time points in group d'. *, P<0.05; **, P<0.01; ***, P<0.001. VEGF, vascular endothelial growth factor; RUNX2, runt-related transcription factor 2; OPG, osteoprotegerin; GAPDH, glyceraldehyde-3-phosphate dehydrogenase; RANKL, receptor activator of nuclear factor-κβ ligand; WB, Western blotting.

after radiation may affect the expression of VEGF related to bone vascular metabolism (*Figures 4-6*) (14). Clinical experts have used hyperbaric oxygen to improve vascular metabolism before and after radiotherapy for the prevention and adjuvant treatment of ORN, achieving a degree of success, which is indirectly in line with our results (15,16). In summary, the reduction of VEGF expression is related to ORN development.

Changes in RUNX2 factor expression in the ORN of the mandible

RUNX2 is a specific transcriptional regulator for the differentiation of mesenchymal stem cells into osteoblasts (17). In our study, HE staining and WB analysis of bone repair-related proteins in the radiation extraction group showed that RUNX2 expression was significantly

© Quantitative Imaging in Medicine and Surgery. All rights reserved.

higher than that in the control and simple tooth extraction groups in the early stage of radiation; RUNX2 expression peaked at 15 days and then gradually decreased. Histomorphological analysis showed manifestations of localized restoration (*Figure 3D*). Therefore, it can be concluded that bone repair and reconstruction peaks 15 days after radiation and that bone hyperplasia gradually decreases after 15 days. In the *in vitro* cytology experiment, the osteoblast cell line (MC3T3-E1) was irradiated with low-dose radiation. The expression of osteogenic differentiation-related genes was significantly increased in the early stage and decreased in the later stage, which further indicates that the effect of radiation on osteoblast differentiation is time dependent (*Figures 4-6*) (18-20). RUNX2 expression in group b' was significantly higher than that in groups a', c', and d' at 45 days after radiation (i.e., 30 days after tooth extraction), indicating that bone repair had occurred in the nonradiation group (b'). However, HE staining results suggested that a large number of osteoblasts adhered to the inner surface of the bone (*Figures 3K,3L,4-6*). It has previously been reported that tissue RUNX2 expression is closely related to VEGF expression (21). After radiation, the VEGF expression in bone tissue was low, resulting in the SD rats in group d' being unable to express sufficient osteogenic differentiation factor RUNX2 in the later stage, which contributed to a lack of bone repair (*Figure 3K,3L*) (21,22). Additionally, at 30 and 45 days, group d' should have shown a high expression of the RUNX2 bone repair factor after tooth extraction but instead showed a significant decrease compared with group c'. The reason for these opposing trends in RUNX2 expression between groups c' and d' in the late stage of radiation is unclear. We speculate that it may be due to the trauma of tooth extraction, which provides a channel for oral bacteria to enter and pass through the inside of the jaw, with the bacteria multiplying in the jaw after irradiation. The ability to resist infection is significantly reduced, and local inflammation spreads, affecting RUNX2 expression and aggravating bone repair barriers (23-26). Clinical application of parathyroid hormone to promote the proliferation of osteoblasts to treat early ORN has achieved good results, demonstrating that osteoblast proliferation disorder is a key contributor to the occurrence and development of mandibular ORN (27).

Changes in OPG and RANKL expression and RANKL:OPG ratio in the ORN of the mandible

RANKL is the ligand of RANK. RANKL belongs to the tumor necrosis factor (TNF) ligand superfamily and regulates the differentiation of osteoblasts and their precursors to T cells, B cells, and megakaryocytes. RANKL activates intracellular signal transduction and promotes the maturation and differentiation of osteoclasts by binding to the RANK receptor expressed on osteoclast precursors (28). In our study, RANKL expression in group d' first increased and then decreased, and the transition time was 30 days. It has been speculated that the trauma of tooth extraction leaves the jaw more susceptible to infection; meanwhile, the decrease in RANKL expression facilitates the transformation of osteoclast progenitor cells into macrophages, which intensifies local tissue inflammation and promotes osteonecrosis (29). OPG is a soluble glycoprotein secreted by mesenchymal-derived cells, such as osteoblasts and BMSCs, which reflects the relative number of osteoblasts to a certain extent. The trend of OPG expression in groups b', c', and d' was roughly consistent with that of RUNX2, suggesting that the proliferation of osteoblasts in group d' was weak in the later stage and that bone repair was inhibited. OPG is a decoy receptor that binds to RANKL with high affinity for disrupting the interaction between RANKL and RANK, effectively inhibiting the differentiation, activation, and maturation of osteoclasts, thereby suppressing bone resorption. The RANKL:OPG ratio reflects the number of osteoclasts developed (*Figures 4-6*) (30). The RANKL:OPG ratio in group d' gradually increased after 30 days and peaked at 45 days. Moreover, the RANKL:OPG ratio was the highest in group d' and was significantly higher than that in the control group, whereas that of group b' was lower than that in the control group, indicating that the osteoclasts in group d' were abnormally activated (*Figure 6*). The changes in RUNX2 expression in each group ran counter to the RANKL:OPG ratio trend. It has been reported that RUNX2 can induce RANKL expression while inhibiting OPG expression and promoting the differentiation of osteoclasts (31). RUNX2 expression is negatively correlated with RANKL:OPG ratio, which is consistent with the results of this study. In summary, the abnormal activation of osteoclasts is related to the decrease in RUNX2 expression.

Cytology has shown that radiation can affect the proliferation, apoptosis, and targeted differentiation of BMSCs and the protein expression of bone metabolism-related factors (14,32). In this experiment, the expressions of VEGF, RUNX2, RANKL, and OPG were closely related to the secretory function of BMSCs. It has been speculated that the occurrence of mandibular ORN may be related to

© Quantitative Imaging in Medicine and Surgery. All rights reserved.

the dysfunction of BMSCs (10,33,34) and that infection is closely related to the occurrence of ORN (26). In the SD rats of group d' of our study, bone metabolism abnormally increased after the bacteria had entered the mandible through the tooth extraction wound, which complicated the analysis of ORN etiology. Further studies are needed to clarify the specific mechanisms underlying the effects of infection on bone metabolism in ORN (26).

Conclusions

To the best of our knowledge, this study is the first to systematically study the dynamic changes of gene expression and morphology related to mandibular ORN bone remodeling. Bone remodeling involves the balance between osteoclast resorption and osteoblast osteogenesis. A high expression of bone formation-related genes and proteins is maintained in the preradiation period. Osteoblasts proliferate actively and dominate bone repair and resorption. The gene and protein expression levels are at a low level. However, after 15 days, bone proliferation decreases gradually, the number of osteoblasts decreases, the number of abnormally activated osteoclasts increases abnormally, the expression of bone resorption-related proteins gradually increases, and bone metabolism becomes imbalanced. During the development of ORN, VEGF expression is low, and blood vessel function and metabolism are impaired. Trauma (tooth extraction) causes oral bacteria to enter the jaw, and infections aggravate and dysregulate bone metabolism, thus eventually precipitating clinical ORN. Our findings clarify the pathogenesis of ORN to some extent. However, this study did not produce direct evidence regarding the effect of tooth extraction on bone metabolism after radiation, and the role of bacteria remains unclear; therefore, further research along this line of inquiry is warranted.

Acknowledgments

Funding: This work was supported by the Natural Science Foundation of Fujian Province (No. 2021J01233), the Medical Innovation Project of Fujian Province (No. 2020CXA036), the Fujian Provincial Financial Health Provincial Special Subsidy Funds (No. BPB-ZXF2021), and the Fujian Provincial Financial Health Provincial Special Subsidy Funds (No. BPB-2023ZXF).

Footnote

Reporting Checklist: The authors have completed the ARRIVE reporting checklist. Available at https://qims.amegroups.com/article/view/10.21037/qims-24-47/rc

Conflicts of Interest: All authors have completed the ICMJE uniform disclosure form (available at https://qims.amegroups.com/article/view/10.21037/qims-24-47/coif). The authors have no conflicts of interest to declare.

Ethical Statement: The authors are accountable for all aspects of the work in ensuring that questions related to the accuracy or integrity of any part of the work are appropriately investigated and resolved. This study was reviewed and approved by the Animal Care and Use Committee of Fujian Medical University. All experiments complied with the relevant regulations of the Experimental Animal Center of Fujian Medical University for the care and use of animals.

Open Access Statement: This is an Open Access article distributed in accordance with the Creative Commons Attribution-NonCommercial-NoDerivs 4.0 International License (CC BY-NC-ND 4.0), which permits the non-commercial replication and distribution of the article with the strict proviso that no changes or edits are made and the original work is properly cited (including links to both the formal publication through the relevant DOI and the license). See: https://creativecommons.org/licenses/by-nc-nd/4.0/.

References

1. Hameed MH, Zafar K, Ghafoor R. Management of oral complications in irradiated head and neck cancer patients: Literature review. IJS Short Rep 2018;3:15-21.
2. Topkan E, Kucuk A, Somay E, Yilmaz B, Pehlivan B, Selek U. Review of Osteoradionecrosis of the Jaw: Radiotherapy Modality, Technique, and Dose as Risk Factors. J Clin Med 2023.
3. Sun Y, Sun KH, Wang G. The ultrastructural study on radiation injuries of the jaws and soft tissues. Zhonghua Kou Qiang Yi Xue Za Zhi 1996;31:147-9.
4. Marx RE, Johnson RP. Studies in the radiobiology of osteoradionecrosis and their clinical significance. Oral Surg Oral Med Oral Pathol 1987;64:379-90.

© Quantitative Imaging in Medicine and Surgery. All rights reserved.

5. Marx RE. Osteoradionecrosis: a new concept of its pathophysiology. J Oral Maxillofac Surg 1983;41:283-8.
6. Delanian S, Lefaix JL. The radiation-induced fibroatrophic process: therapeutic perspective via the antioxidant pathway. Radiother Oncol 2004;73:119-31.
7. Zong C, Cai B, Wen X, Alam S, Chen Y, Guo Y, Liu Y, Tian L. The role of myofibroblasts in the development of osteoradionecrosis in a newly established rabbit model. J Craniomaxillofac Surg 2016;44:725-33.
8. Xu J, Zheng Z, Fang D, Gao R, Liu Y, Fan ZP, Zhang CM, Wang SL. Early-stage pathogenic sequence of jaw osteoradionecrosis in vivo. J Dent Res 2012;91:702-8.
9. Bléry P, Espitalier F, Hays A, Crauste E, Demarquay C, Pilet P, Sourice S, Guicheux J, Malard O, Benderitter M, Weiss P, Mathieu N. Development of mandibular osteoradionecrosis in rats: Importance of dental extraction. J Craniomaxillofac Surg 2015;43:1829-36.
10. Tatsuyama K, Maezawa Y, Baba H, Imamura Y, Fukuda M. Expression of various growth factors for cell proliferation and cytodifferentiation during fracture repair of bone. Eur J Histochem 2000;44:269-78.
11. Carmeliet P, Ferreira V, Breier G, Pollefeyt S, Kieckens L, Gertsenstein M, Fahrig M, Vandenhoeck A, Harpal K, Eberhardt C, Declercq C, Pawling J, Moons L, Collen D, Risau W, Nagy A. Abnormal blood vessel development and lethality in embryos lacking a single VEGF allele. Nature 1996;380:435-9.
12. Deshpande SS, Donneys A, Farberg AS, Tchanque-Fossuo CN, Felice PA, Buchman SR. Quantification and characterization of radiation-induced changes to mandibular vascularity using micro-computed tomography. Ann Plast Surg 2014;72:100-3.
13. Verdonck HW, Meijer GJ, Laurin T, Nieman FH, Stoll C, Riediger D, Stoelinga PJ, de Baat C. Assessment of vascularity in irradiated and nonirradiated maxillary and mandibular minipig alveolar bone using laser doppler flowmetry. Int J Oral Maxillofac Implants 2007;22:774-8.
14. Sun R, Zhu G, Wang J, Tong L, Zhai J. Indirect effects of X-irradiation on proliferation and osteogenic potential of bone marrow mesenchymal stem cells in a local irradiated rat model. Mol Med Rep 2017;15:3706-14.
15. Svalestad J, Thorsen E, Vaagbø G, Hellem S. Effect of hyperbaric oxygen treatment on oxygen tension and vascular capacity in irradiated skin and mucosa. Int J Oral Maxillofac Surg 2014;43:107-12.
16. Corrao G, Mazzola GC, Lombardi N, Marvaso G, Pispero A, Baruzzi E, et al. Oral Surgery and Osteoradionecrosis in Patients Undergoing Head and Neck Radiation Therapy: An Update of the Current Literature. Biomedicines 2023;11:3339.
17. Zheng H, Guo Z, Ma Q, Jia H, Dang G. Cbfa1/osf2 transduced bone marrow stromal cells facilitate bone formation in vitro and in vivo. Calcif Tissue Int 2004;74:194-203.
18. Szymczyk KH, Shapiro IM, Adams CS. Ionizing radiation sensitizes bone cells to apoptosis. Bone 2004;34:148-56.
19. Nepon H, Safran T, Reece EM, Murphy AM, Vorstenbosch J, Davison PG. Radiation-Induced Tissue Damage: Clinical Consequences and Current Treatment Options. Semin Plast Surg 2021;35:181-8.
20. He J, Qiu W, Zhang Z, Wang Z, Zhang X, He Y. Effects of irradiation on growth and differentiation-related gene expression in osteoblasts. J Craniofac Surg 2011;22:1635-40.
21. Berendsen AD, Olsen BR. How vascular endothelial growth factor-A (VEGF) regulates differentiation of mesenchymal stem cells. J Histochem Cytochem 2014;62:103-8.
22. Han B, Yang Z, Nimni M. Effects of gamma irradiation on osteoinduction associated with demineralized bone matrix. J Orthop Res 2008;26:75-82.
23. Pierce JL, Begun DL, Westendorf JJ, McGee-Lawrence ME. Defining osteoblast and adipocyte lineages in the bone marrow. Bone 2019;118:2-7.
24. Koga DH, Salvajoli JV, Alves FA. Dental extractions and radiotherapy in head and neck oncology: review of the literature. Oral Dis 2008;14:40-4.
25. Cohen M, Nishimura I, Tamplen M, Hokugo A, Beumer J, Steinberg ML, Suh JD, Abemayor E, Nabili V. Animal model of radiogenic bone damage to study mandibular osteoradionecrosis. Am J Otolaryngol 2011;32:291-300.
26. Gilbert LC, Chen H, Lu X, Nanes MS. Chronic low dose tumor necrosis factor-α (TNF) suppresses early bone accrual in young mice by inhibiting osteoblasts without affecting osteoclasts. Bone 2013;56:174-83.
27. Chandra A, Lin T, Tribble MB, Zhu J, Altman AR, Tseng WJ, Zhang Y, Akintoye SO, Cengel K, Liu XS, Qin L. PTH1-34 alleviates radiotherapy-induced local bone loss by improving osteoblast and osteocyte survival. Bone 2014;67:33-40.
28. Lacey DL, Timms E, Tan HL, Kelley MJ, Dunstan CR, Burgess T, et al. Osteoprotegerin ligand is a cytokine that regulates osteoclast differentiation and activation. Cell 1998;93:165-76.
29. Morita M, Iwasaki R, Sato Y, Kobayashi T, Watanabe R, Oike T, Nakamura S, Keneko Y, Miyamoto K, Ishihara K, Iwakura Y, Ishii K, Matsumoto M, Nakamura M,

© Quantitative Imaging in Medicine and Surgery. All rights reserved.

Kawana H, Nakagawa T, Miyamoto T. Elevation of pro-inflammatory cytokine levels following anti-resorptive drug treatment is required for osteonecrosis development in infectious osteomyelitis. Sci Rep 2017;7:46322.
30. Naumnik B, Klejna K, Koc-Żórawska E, Myśliwiec M. Age and gender predict OPG level and OPG/sRANKL ratio in maintenance hemodialysis patients. Adv Med Sci 2013;58:382-7.
31. Enomoto H, Shiojiri S, Hoshi K, Furuichi T, Fukuyama R, Yoshida CA, Kanatani N, Nakamura R, Mizuno A, Zanma A, Yano K, Yasuda H, Higashio K, Takada K, Komori T. Induction of osteoclast differentiation by Runx2 through receptor activator of nuclear factor-kappa B ligand (RANKL) and osteoprotegerin regulation and partial rescue of osteoclastogenesis in Runx2-/- mice by RANKL transgene. J Biol Chem 2003;278:23971-7.
32. Lee JS, Lee JM, Im GI. Electroporation-mediated transfer of Runx2 and Osterix genes to enhance osteogenesis of adipose stem cells. Biomaterials 2011;32:760-8.
33. Baud'huin M, Duplomb L, Teletchea S, Lamoureux F, Ruiz-Velasco C, Maillasson M, Redini F, Heymann MF, Heymann D. Osteoprotegerin: multiple partners for multiple functions. Cytokine Growth Factor Rev 2013;24:401-9.
34. Jin IG, Kim JH, Wu HG, Kim SK, Park Y, Hwang SJ. Effect of bone marrow-derived stem cells and bone morphogenetic protein-2 on treatment of osteoradionecrosis in a rat model. J Craniomaxillofac Surg 2015;43:1478-86.

Cite this article as: Liu S, Zhang B, Ma S, Wu F, Shi X, Wu J, Jensen OT, Cariati P, Hong J, Zhu X. The mechanism of bone metabolism in a Sprague Dawley rat model of mandibular osteoradionecrosis. Quant Imaging Med Surg 2024. doi: 10.21037/qims-24-47

© Quantitative Imaging in Medicine and Surgery. All rights reserved.